

## Preparation of a composite membrane made of PoPD/PVA ultrafiltration layer on ceramic pozzolan/micronized phosphate support for removal of Congo red dye

Dounia Beqqour<sup>a,\*</sup>, Wiame Taanaoui<sup>a</sup>, Ghizlane Derouich<sup>a</sup>, Mohamed Ouammou<sup>a</sup>, Saad Alami Younssi<sup>a</sup>, Jamal Bennazha<sup>a</sup>, Jason A. Cody<sup>b</sup>

<sup>a</sup>Laboratory of Materials, Membranes and Environment, Faculty of Sciences and Technologies Mohammedia, University Hassan II of Casablanca, Morocco, emails: dounia.beqqour-etu@etu.univh2c.ma (D. Beqqour), wiametaanaoui@gmail.com (W. Taanaoui), gh.derouich@gmail.com (G. Derouich), mouammou@yahoo.fr (M. Ouammou), alamiyounssisaad@yahoo.fr (S.A. Younssi), jbenmazha@yahoo.fr (J. Bennazha)

<sup>b</sup>Department of Chemistry, Lake Forest College, 555 N. Sheridan Rd., Lake Forest, IL, USA, email: cody@mx.lakeforest.edu

Received 23 October 2021; Accepted 20 December 2021

### ABSTRACT

This work presents the development of a composite ultrafiltration membrane based on poly(o-phenylenediamine) and poly(vinyl alcohol) on flat ceramic support made from pozzolan and micronized phosphate. The active layer was coated on the ceramic support using the dip-coating technique. The developed membrane was characterized by Fourier-transform infrared spectroscopy, water contact angle, permeability, scanning electron microscopy, energy-dispersive X-ray analysis, pore size, as well as filtration performance. The ultrafiltration membrane has a pore diameter of 45 nm, a water permeability of 37.28 L/h m<sup>2</sup> bar and a water contact angle of 50°. Finally, the performance of the composite membrane was assessed by the filtration of Congo red dye by varying the operating conditions including the applied pressure (1–3 bar), the feed concentration (20–600 ppm) as well as the feed pH (4–10). The membrane is highly effective for removal of soluble Congo red dye: the rejection was 99.79% under a pressure of 3 bar, a concentration of 600 ppm and a pH of 4.

**Keywords:** Composite membrane; Poly(o-phenylenediamine); Poly(vinyl alcohol); Pozzolan/micronized phosphate; Ultrafiltration; Congo red dye

### 1. Introduction

Currently, water scarcity is fast becoming a global emergency as consumable water resources are limited while both population and water needs are growing. Furthermore, water pollution exacerbates this growing water shortage [1]. The increased demand for antiseptic water and water treatment therefore requires research, application and continuous improvement of water treatment processes [2]. The textile industry adds beauty to clothes and home furnishings, but uses dyes that are among the many pollutants in water [3]. Textile wastewater treatment is a challenge

due to its high pH, high temperature, high chemical oxygen demand as well as the low biodegradability of many dyes. The wastewater contains high concentrations of azo dyes and inorganic salts which can affect human health and the environment [4], and therefore must be treated before being reintroduced to natural bodies of water.

Synthetic dyes are largely non-degradable [5], due to their stable and complex chemical components [6]. Research to date includes the use of different water treatment techniques such as coagulation [7], flocculation [8], adsorption [9], precipitation [10] and oxidation [11]. Nonetheless, most of the methods mentioned above struggle to completely

\* Corresponding author.

remove residual dyes and salts [4]. Hence, membrane technology involving microfiltration [12], ultrafiltration (UF) [13], nanofiltration [14] and reverse osmosis [15] has gained attention due to its cost-effectiveness, simplicity, high separation efficiency, accessible operating conditions, and environmental compatibility [16].

Currently, UF is a well-recognized membrane process [2], established as the most cost-effective and sustainable wastewater technology [17]. As a result, it attracts growing interest for dye removal [18]. Currently, UF membranes are widely used in different industries and fields including chemical, pharmaceutical, food, petroleum, metallurgy, biology, environmental remediation and water treatment [19].

Commercially available polymers for UF membranes include polysulfone [20], cellulose acetate [21], polyethersulfone [22] and polyacrylonitrile [23]. However, the chemical resistance and anti-fouling properties of these polymeric membranes reduce the permeation flux, influence the efficiency and shorten the life of the membranes [24].

Recently, ceramic membranes have attracted significant research interest because of their good mechanical and chemical stabilities [25,26]. For instance, ceramic membranes made from industrial metal oxides such as titania, zirconia, silica and alumina are highly robust but are also quite expensive [27]. For this reason, using low-cost alternative materials stimulated much interest [28]. Among these materials, bentonite, perlite and phosphate are successfully employed in the preparation of low-cost ceramic membranes [28–29].

Thus, the current work investigates Congo red (CR) removal using a new UF composite membrane (CM) made of a mixture of poly(*o*-phenylenediamine) (PoPD) and poly(vinyl alcohol) (PVA) that was deposited on a flat ceramic support made from pozzolan incorporated with micronized phosphate (Pz-MP). The PoPD was widely used in many applications such as removal and photodegradation of inorganic and organic pollutants dissolved in water [30]. Furthermore, PoPD is one of the aniline derivatives which has gained increased attention owing to its stability and is widely used for removal of Pb(II), Hg(II) and Cr(VI) [31–33]. One of the main reasons for using PVA is the fact that it can potentially minimize fouling rates due to its oleophobic nature [34]. Besides, it has good cohesion, biocompatibility, hydrophilicity as well as biodegradability. PVA will allow the preparation of a chemically, thermally and mechanically resistant membrane with a thin homogeneous layer. In addition, the dense network structure of the PVA will embed and constrain PoPD into the network. The aim of this work is to combine the properties of both PoPD and PVA to obtain a selective layer that will be used in ultrafiltration application.

Pozzolan and micronized phosphate were selected as raw materials for the preparation of the ceramic support due to the interesting attributes of this support as mentioned in our previous study [28].

Several characterizations were used in order to evaluate the morphology, hydrophobicity, and filtration efficiency of the CM. Techniques included Fourier-transform infrared spectroscopy (FTIR), scanning electron microscopy (SEM), energy-dispersive X-ray analysis (EDX), pore size and water contact angle measurements (WCA). Also, the membrane performance for filtration of CR dye was evaluated using

tangential filtration. The effects of the operating pressure, the feed concentration and the feed pH on permeation and rejection of CR dye using the PoPD-PVA/Pz-MP UF membrane were investigated in detail. Finally, the anti-fouling properties of the developed membrane were also evaluated.

## 2. Experimental

### 2.1. Materials

Flat ceramic support (Pz/MP) elaborated as previously mentioned was used for deposition of the selective PoPD/PVA layer [28].

The monomer *o*-phenylenediamine (oPD) and the ammonium persulfate (APS, 98%) were purchased from Sigma-Aldrich and Loba Chemie, respectively. The PVA (RHODOVIOL 25/140) was obtained from Prolabo. The hydrochloric acid (HCl, 37%) was purchased from VWR Chemicals. CR dye (35%) was obtained from Sigma-Aldrich. More information and properties of CR dye are presented in Table 1.

### 2.2. Chemical polymerization of the oPD

PoPD was synthesized by chemical polymerization. The oxidant APS was dissolved in HCl (0.5 M) and added dropwise to the oPD monomer under continuous stirring. Next, to assure complete polymerization, the solution was stirred for an additional 6 h. Then, the suspended solid (PoPD) was recovered by filtration, washed with distilled water and dried in an oven at 60°C overnight [35].

### 2.3. Preparation of the PoPD-PVA/Pz-MP membrane

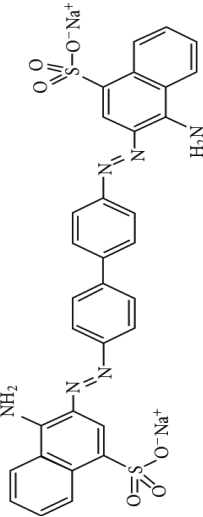
The preparation process of the membrane is as follows: First, the flat Pz/MP ceramic support was cleaned with water via ultrasound irradiation for 20 min to remove residual particles and then dried overnight at 100°C. Then, the PoPD powder was added to a prepared PVA solution (10 wt.% of PVA in water). The mixture was stirred until the solution was homogeneous. The resulting mass ratio of PoPD/PVA is 0.47 [35,36]. Finally, the resulting solution was dip-coated onto the ceramic support under atmospheric conditions, left for 1 h and dried for 24 h at 60°C [35,36]. The obtained PoPD-PVA/Pz-MP membrane was then thoroughly characterized and evaluated as described in subsequent sections.

### 2.4. UF experiments

UF experiments were performed using a stainless-steel laboratory pilot system. It contains a storage tank of 5 L supplied by a circulation pump where the pressure is provided by an air compressor. This operating pressure crosses a membrane surface of 4.52 cm<sup>2</sup> and is controlled by a pressure regulator. It should be noted that during the UF tests, the feed solution was maintained at room temperature by means of a cooling system. The schematic UF system is depicted in Fig. 1.

At different operating pressures varied from 1 to 3 bar, the water permeability of the developed membrane was

Table 1  
Characteristics of CR dye

| Identification  |         | Chemical properties         |  | Physical properties      |          |                                  |
|---|---------|-----------------------------|--|--------------------------|----------|----------------------------------|
| Nomenclature/synonym  | Type    | Chemical formula            | Chemical structure   | Molecular weight (g/mol) | pKa      | Wavelength $\lambda_{\max}$ (nm) |
| <ul style="list-style-type: none"> <li>disodium 4-amino-3-[4-[4-(1-amino-4-sulfonato-naphthalen-2-yl)diazenyl]phenyl]phenyl] diazenyl-naphthalene-1-sulfonate</li> <li>Direct Red 28</li> </ul> | Anionic | $C_{32}H_{22}N_6Na_2O_6S_2$ |  | 696.66                   | Around 4 | 499                              |

measured. Permeate flux  $J_w$  (L/h m<sup>2</sup>) and the permeability  $L_p$  (L/h m<sup>2</sup> bar) through the membrane are expressed by Eqs. (1) and (2), respectively.

$$J_w = \frac{V}{A \cdot t} \quad (1)$$

$$L_p = \frac{J_w}{\Delta P} \quad (2)$$

where  $V$  (L) is total permeate collected crosses the membrane surface,  $A$  (m<sup>2</sup>) during interval time  $t$  (h) and  $\Delta P$  is the applied pressure (bar).

The separation performance of PoPD-PVA/Pz-MP membrane toward CR dye was tested on different operating pressures ranging from 1 to 3 bar, different feed concentrations of CR dye (20–600 ppm) and at varying pH (4–10). The feed pH was adjusted by adding drops of HCl (2 M) and NaOH (2 M) solutions. The permeate was collected to determine the dye removal factor by membrane filtration. Eq. (3) is used to calculate the rejection  $R$  (%) of CR dye solution by the PoPD-PVA/Pz-MP membrane:

$$R = \left( 1 - \frac{C_{\text{permeate}}}{C_{\text{feed}}} \right) \times 100 \quad (3)$$

where  $C_{\text{permeate}}$  and  $C_{\text{feed}}$  are respectively the concentration of the permeate and the feed (ppm).

### 2.5. Antifouling study

In order to study the antifouling properties, the initial water permeate flux ( $J_{w0}$  L/h m<sup>2</sup>) through the UF membrane was measured at an operating pressure of 3 bar over 2 h of filtration. Under the same operational conditions, the flux ( $J_p$  L/h m<sup>2</sup>) was measured at CR concentration of 600 ppm.

After rinsing the membrane with distilled water for 60 min using the UF pilot, the water permeate flux ( $J_{w1}$  L/h m<sup>2</sup>) was measured again.

PoPD-PVA/Pz-MP membrane fouling resistance was estimated by the flux recovery ratio (FRR) using Eq. (4) [2]:

$$FRR = \frac{J_{w1}}{J_{w0}} \times 100 \quad (4)$$

Overall, fouling achievement was examined by total flux decline ratio (TFR) and reversible flux decline ratio (RFR) using Eqs. (5) and (6), respectively [37]:

$$TFR = \left( 1 - \frac{J_p}{J_{w0}} \right) \times 100 \quad (5)$$

$$RFR = \frac{J_{w1} - J_p}{J_{w0}} \times 100 \quad (6)$$

The irreversible flux decline ratio (IFR) of the developed membrane was computed using Eq. (7) [34]:

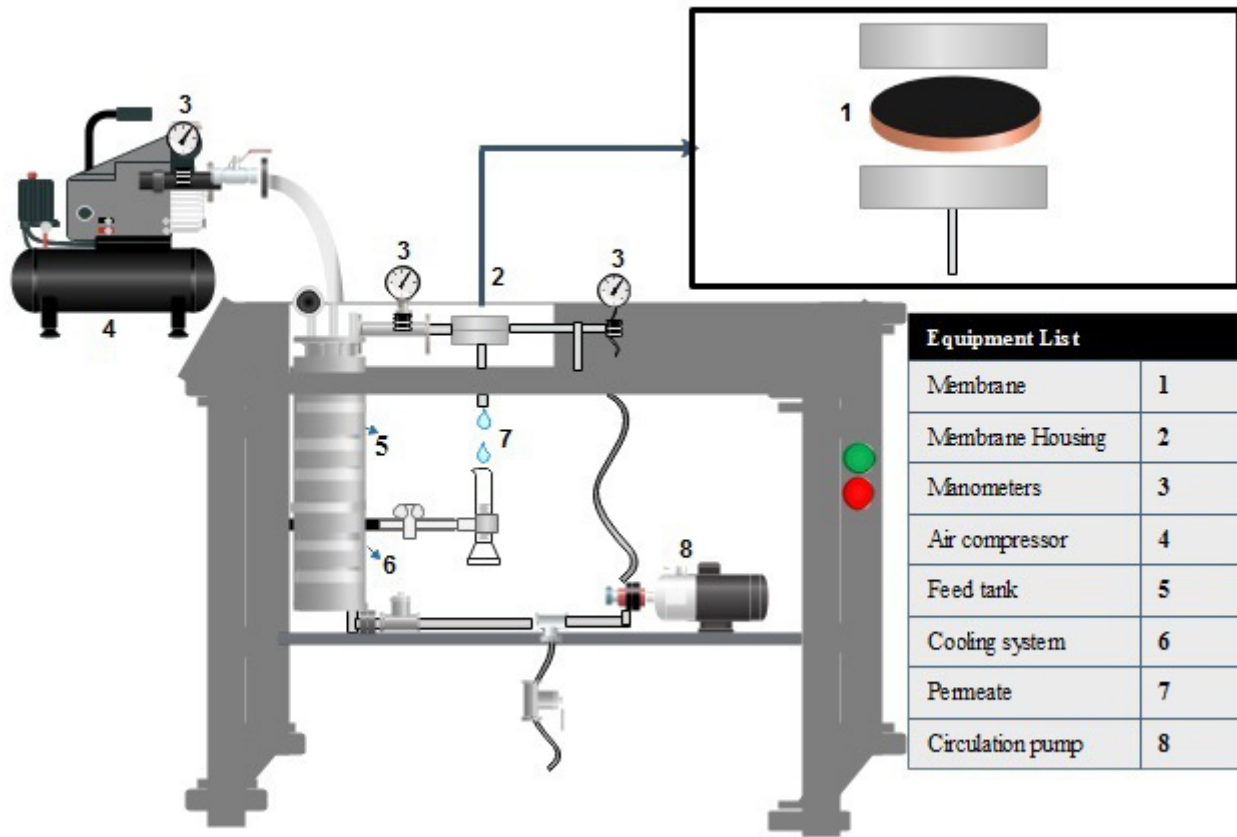


Fig. 1. Scheme of UF pilot system.

$$\text{IFR} = \frac{J_{w0} - J_{w1}}{J_{w0}} \times 100 \quad (7)$$

### 2.6. Membrane characterization

FTIR spectra of the PoPD, PVA and the PoPD/PVA membrane layer (peeled off the ceramic support) were conducted on a Bruker Spectrometer (VERTEX 70). The WCA for the Pz/MP support and the PoPD-PVA/Pz-MP membrane was measured using a Digidrop Goniometer (GBX-Instruments). An SEM operating at 10 kV (FEI Company, Quanta 200) was used for membrane morphology observations of the surfaces of both the Pz/MP support and the PoPD-PVA/Pz-MP membrane as well as the cross section of the membrane. The elemental composition of the developed membrane was determined using the EDX detector on the SEM.

The average pore size was calculated using the extended Hagen–Poiseuille equation [Eq. (8)] [28]:

$$d = 2 \sqrt{\frac{8 J_w \cdot \delta \cdot \tau \cdot \Delta X}{\varepsilon \Delta P}} \quad (8)$$

where  $d$  (m) is the pore diameter,  $J_w$  (m/s) is the water flux,  $\delta$  (Pa·s) is the water viscosity,  $\tau$  is the tortuosity factor (2.5 for sphere particle packing),  $\varepsilon$  (%) is the porosity of the

membrane,  $\Delta P$  (Pa) is the applied pressure, and  $\Delta X$  (m) is the membrane thickness.

The pH of the solution was measured using a pH meter (METTLER TOLEDO SevenCompact pH/Ion). The concentration of CR dye before and after filtration was measured by a UV-Vis Spectrophotometry (JASCO V-730 Spectrophotometer) at a maximum absorbance wavelength of 499 nm using quartz cells. The determination of point of zero charge (PZC) of PoPD-PVA/Pz-MP membrane was carried out by the solid addition method as described elsewhere [38].

## 3. Results and discussion

### 3.1. Characterization of the PoPD-PVA/Pz-MP membrane

#### 3.1.1. FTIR analysis

The FTIR spectra of the PVA, PoPD, and PoPD/PVA layer are shown in Fig. 2. Starting with PVA, the highest band intensity in the region of  $3,280 \text{ cm}^{-1}$  is associated with the O–H stretching vibration of the hydroxy group [39,40]. The peak at  $2,917 \text{ cm}^{-1}$  is attributed to  $\text{CH}_2$  asymmetric stretching vibration [40], while the very small peak at  $1,718 \text{ cm}^{-1}$  is due to the C=O vibration [41]. The peak at  $1,425 \text{ cm}^{-1}$  is linked to C–H bending vibration of  $\text{CH}_2$  [40] whereas the peak at  $1,324 \text{ cm}^{-1}$  is attributed to C–H deformation vibration [39]. The peak at  $1,081 \text{ cm}^{-1}$  corresponds to C–O stretching of

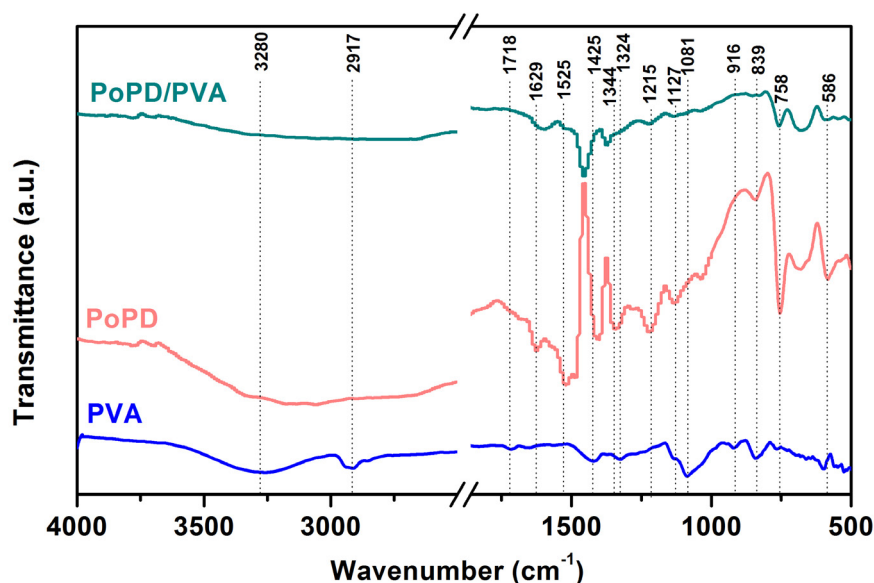


Fig. 2. FTIR spectra of PVA, PoPD and PoPD/PVA membrane layer.

acetyl groups [40] while the peak at  $916\text{ cm}^{-1}$  is due to  $\text{CH}_2$  rocking [40]. The last peak at  $839\text{ cm}^{-1}$  is assigned to C–C stretching [39].

For the PoPD, peaks at  $1,629$  and  $1,525\text{ cm}^{-1}$  are associated with the stretching vibrations of C=C and C=N group in the phenazine ring [42–44]. The peaks at  $1,344$  and  $1,215\text{ cm}^{-1}$  are associated with C–N–C stretching in the benzenoid and quinoid imine units [33,42,44], while the band at  $1,127\text{ cm}^{-1}$  can be related to the C–N–C stretching bond [45]. The presence of the bands appearing at  $758$  and  $586\text{ cm}^{-1}$  are characteristic of the C–H out-of-plane bending vibrations of benzene nuclei in the phenazine skeleton [43].

In the spectrum corresponding to the PoPD/PVA membrane layer, there are some peaks that correspond to the PoPD which are the peaks located at  $1,525$ ;  $1,215$ ;  $758$  and  $586\text{ cm}^{-1}$ . There is also a peak that correspond to the PVA which is the peak located at  $839\text{ cm}^{-1}$ .

Furthermore, the spectrum contains two peaks that are shifted towards longer wavenumber. The first peak corresponds to the PVA and was located at  $1,425\text{ cm}^{-1}$ , is linked to C–H bending vibration. The second peak that was at  $1,344\text{ cm}^{-1}$  corresponds to the PoPD and is associated with C–N–C stretching in the benzenoid imine units.

### 3.1.2. Water contact angle measurement

In order to study the surface hydrophilicity of the Pz/MP support as well as the PoPD-PVA/Pz-MP membrane, the WCA was measured. The obtained values are presented in Fig. 3. As observed, WCA of the ceramic support and the developed membrane is measured to be  $21^\circ$  and  $50^\circ$ , respectively. The lower value obtained of the support means that its surface has a higher hydrophilic character which is highly due to the porous morphology of the Pz/MP support. Compared to the bare support, the WCA of the PoPD-PVA/Pz-MP membrane increases to  $50^\circ$ , meaning that the membrane surface becomes less hydrophilic.

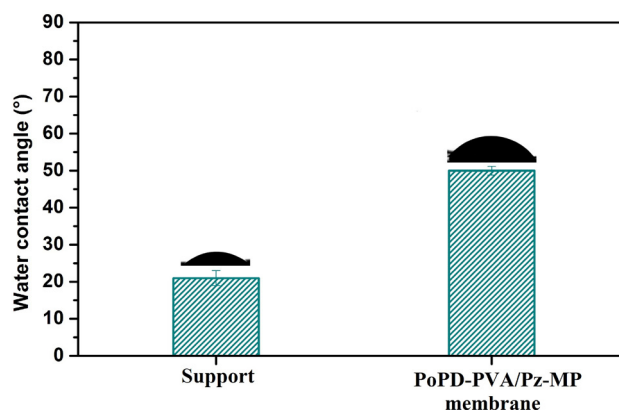


Fig. 3. WCA of Pz/MP support and PoPD-PVA/Pz-MP membrane.

This variation in WCA is due to the use of a hydrophobic component which is PVA in the membrane layer.

### 3.1.3. Permeability

Fig. 4 depicts the permeate flux (of water) as a function of the operating pressure of the PoPD-PVA/Pz-MP membrane. As expected, the water permeate flux increases linearly with an increase of applied pressure and follows Darcy's law. The slope in this figure gives a permeability value equal to  $37.28\text{ L/h m}^2\text{ bar}$ .

### 3.1.4. SEM observation

The SEM images of the top-views for both the Pz/MP support and the PoPD-PVA/Pz-MP membrane, as well as the cross section of the CM are depicted in Fig. 5. The Pz/MP support surface is highly porous and crack

free (Fig. 5a). Fig. 5b shows the deposition of PoPD and PVA onto the surface of the membrane. The developed membrane has a homogenous surface with a spherical morphology due to the PoPD particles [31]. Fig. 5c shows the cross-section of the PoPD-PVA/Pz-MP membrane revealing a rather uniform layer deposition of 72.85  $\mu\text{m}$  in thickness (determined from the average of measured

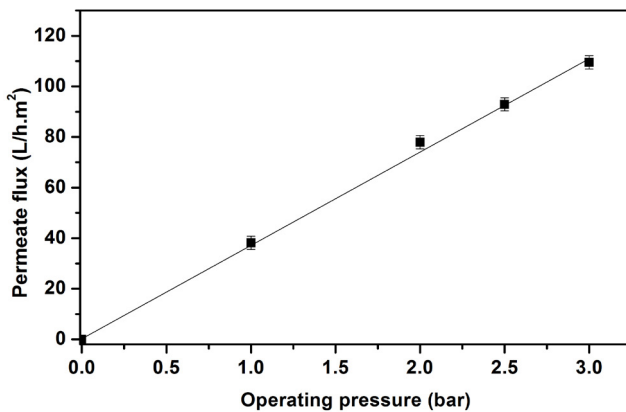


Fig. 4. Permeate flux as a function of operating pressure of the PoPD-PVA/Pz-MP membrane.

values) on the Pz/MP support. Two measurements are shown in green: the full polymer layer thickness of 73.06  $\mu\text{m}$  and then the sum of the dense (PVA) and less dense (PoPD) portions of the polymer layer ( $41.09 + 31.56 = 72.65 \mu\text{m}$ ).

### 3.1.5. EDX analysis

Fig. 6 depicts the EDX spectrum of the PoPD-PVA/Pz-MP membrane, which quantitatively detects the constituent elements. The PoPD is a compound composed of C and N, and the PVA contains C and O. The spectrum shows carbon (C), oxygen (O) and nitrogen (N) peaks with weight percent of 52.06, 25.41 and 20.27 wt.%, respectively. Some O might also be detected from the ceramic support. The other peaks detected in the EDX spectrum including sulfur (S) and chlorine (Cl) are attributed to the chemical composition of the Pz/MP support. The expected elemental compositions are found in the EDX spectrum and confirm that the PoPD and PVA are deposited on the ceramic support.

### 3.1.6. Pore size

The pore size of the PoPD-PVA/Pz-MP membrane was calculated and found to be 45 nm. This means that the developed membrane could be used for UF applications such as removal of organic soluble dyes.

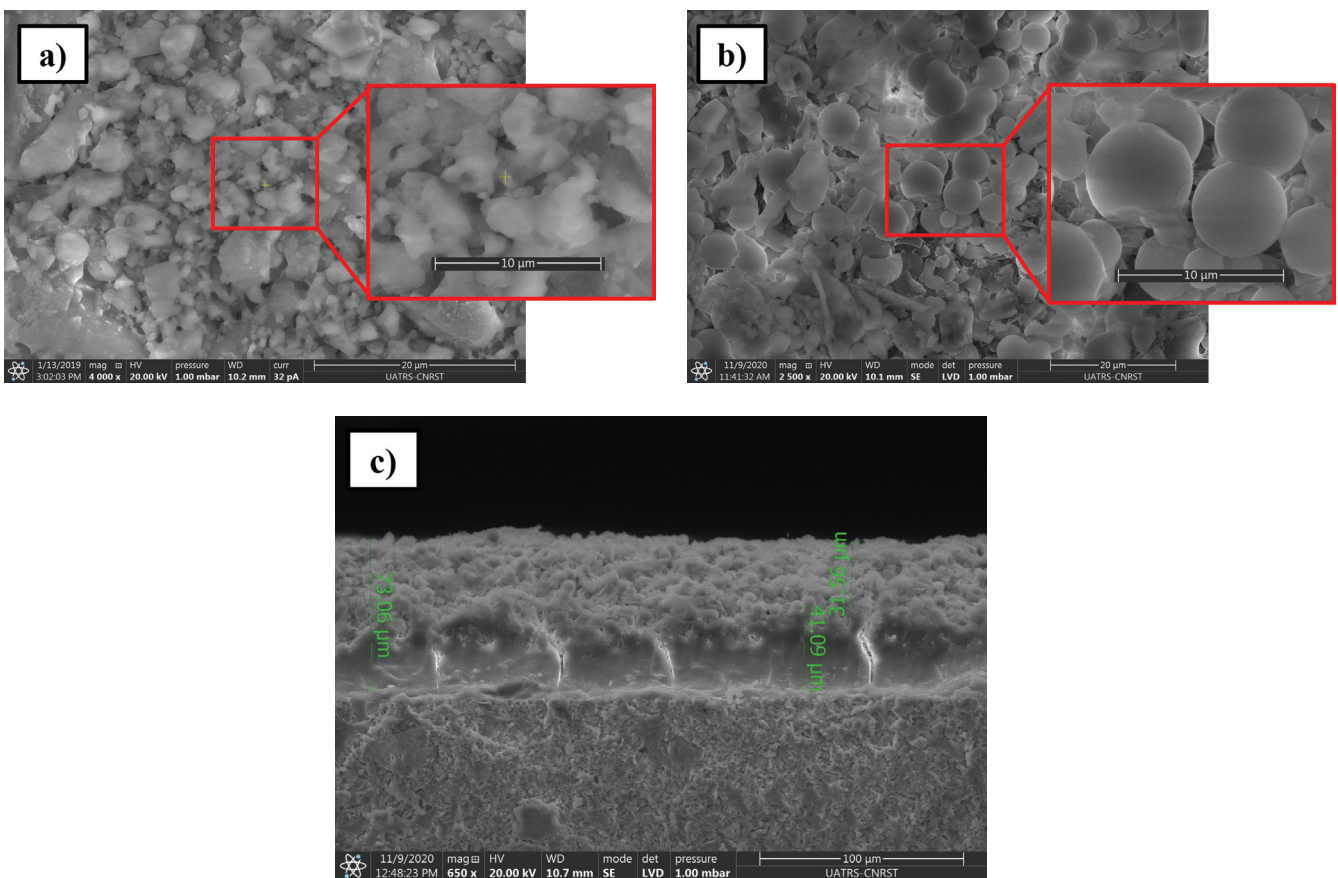


Fig. 5. SEM micrographs of (a) the top-view of the Pz/MP support, (b) the PoPD-PVA/Pz-MP membrane and (c) the cross-section of the CM.

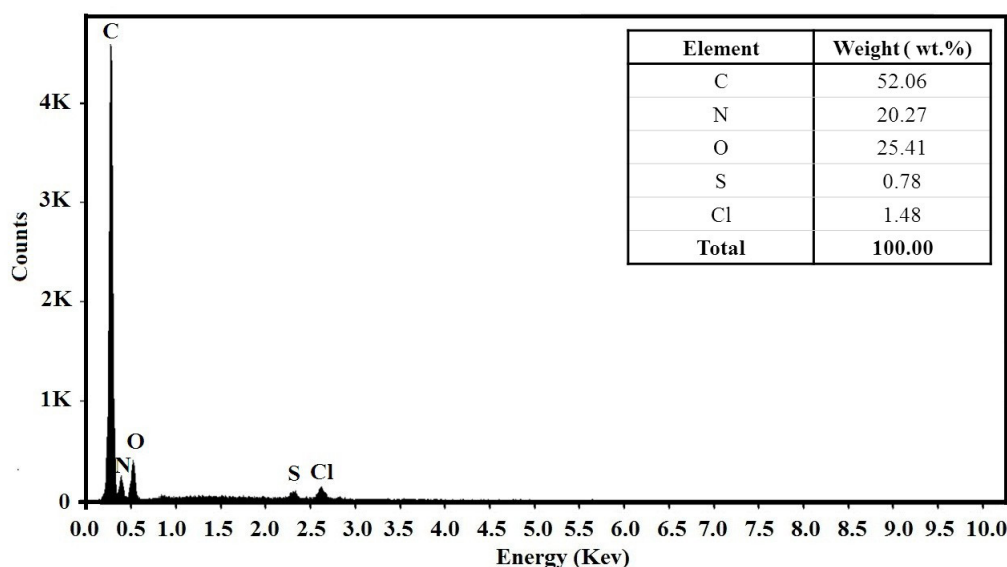


Fig. 6. EDX spectrum of PoPD-PVA/Pz-MP membrane.

### 3.2. UF experiments

In order to assess the applicability of PoPD-PVA/Pz-MP membrane in the separation of CR dye, its filtration behavior was investigated. This study is conducted to examine the effects of different parameters on the membrane performance involving the operating pressure, the feed concentration and the feed pH.

#### 3.2.1. Effect of operating pressure

The permeate flux values and percentage of CR dye rejection as a function of operating pressure are displayed in Fig. 7. During 2 h of filtration, the effect of applied pressure (1–3 bar) on dye rejection was assessed at a fixed concentration of 20 ppm and a feed pH around 6.72 which is approximately the  $\text{pH}_{\text{PZC}}$  determined experimentally of the membrane ( $\text{pH}_{\text{PZC}} = 6.72$ ).

The permeate flux increased slightly with the increase of operating pressures (Fig. 7a), ranging from as low as 20 L/h m<sup>2</sup> at 1 bar up to 35.62 L/h m<sup>2</sup> at 3 bar. Overall, higher operating pressures gave an increase in permeate flux. Knowing that the filtration through a membrane is a pressure-driven physical process, this increase in flux can be explained by an increase in driving force [46]. Besides, the permeate flux is less than water permeate flux. This reduction in permeate flux might be due to membrane fouling if the dye particles were adsorbed on the active surface of the PoPD-PVA/Pz-MP membrane or settled into pores [47]. Furthermore, the CR rejection (Fig. 7b) was nearly constant even at higher operating pressure (the rejection is 97.01% at 1 bar and 97.75% at 3 bar), meaning that the effect of applied pressure on the rejection appears negligible, which implies that the dye elimination is mainly due to electrostatic interactions [48]. Based on the higher permeate flux and the similar percentage of dye

rejection, the operating pressure of 3 bar is considered as the optimal applied pressure for CR filtration.

#### 3.2.2. Effect of feed concentration

The filtration performance of PoPD-PVA/Pz-MP membrane on the permeate flux and rejection, was assessed at different concentrations (20–600 ppm) of CR dye (Fig. 8), under a constant operating pressure of 3 bar and a pH value around 6.72. As anticipated, the permeate flux dropped with increasing concentrations of CR dye which raises the membrane fouling [49]. It is clearly seen from Fig. 8a that the permeate flux decreases from 35.62 to 12.39 L/h m<sup>2</sup> while increasing the CR concentration. This can be ascribed to the adsorption of the dye on the membrane surface [29], or incorporation into the pores resulting in a decrease of the permeate flux. It can also be due to the increase in concentration polarization [49].

As indicated in Fig. 8b, over 2 h of filtration, CR dye removal of 97.75% and 98.66% was achieved at feed concentrations of 20 and 600 ppm, respectively. The rejection remained high and relatively constant over this range of dye concentration [46,49]. The rejected dye likely accumulated on the surface, forming a polarization layer that can be considered as an additional contribution to CR dye filtration [29]. Whereas diffusion is the dominant mode of transport within this polarization layer [50], electrostatic repulsion may be responsible for the increase in dye rejection rate as each CR dye molecule has two negatively charged sulfonate groups. In addition, the rejection of the dye is enhanced by electrostatic repulsion effects due to the formation of clusters of CR dye with multiple charges [51,52].

#### 3.2.3. Effect of feed pH

Solution pH could affect the permeate flux as well as the rejection rate, which in turn influences the membrane

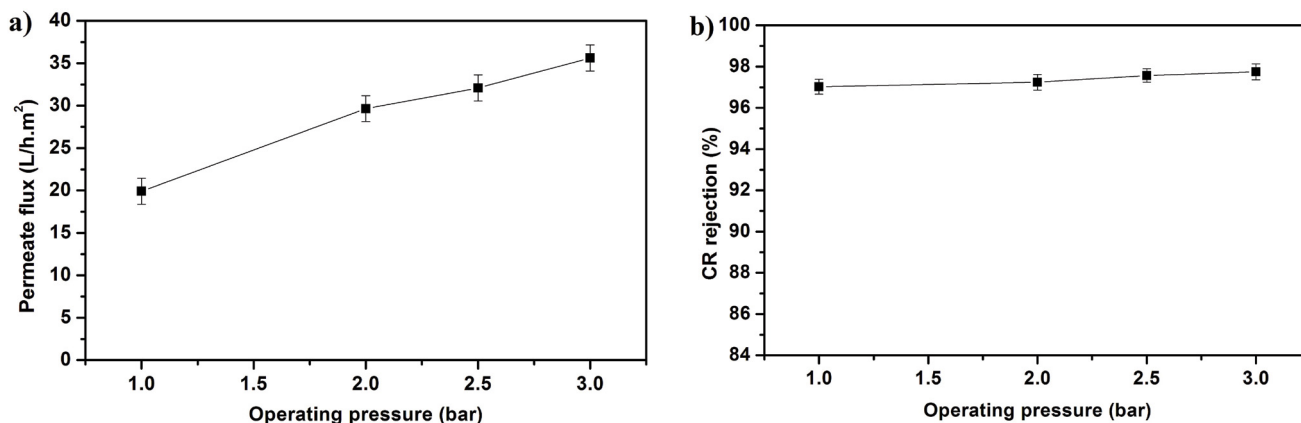


Fig. 7. CR permeate flux (a) and rejection (b) as a function of operating pressure at  $C = 20$  ppm and  $\text{pH} = 6$  for 2 h of filtration.

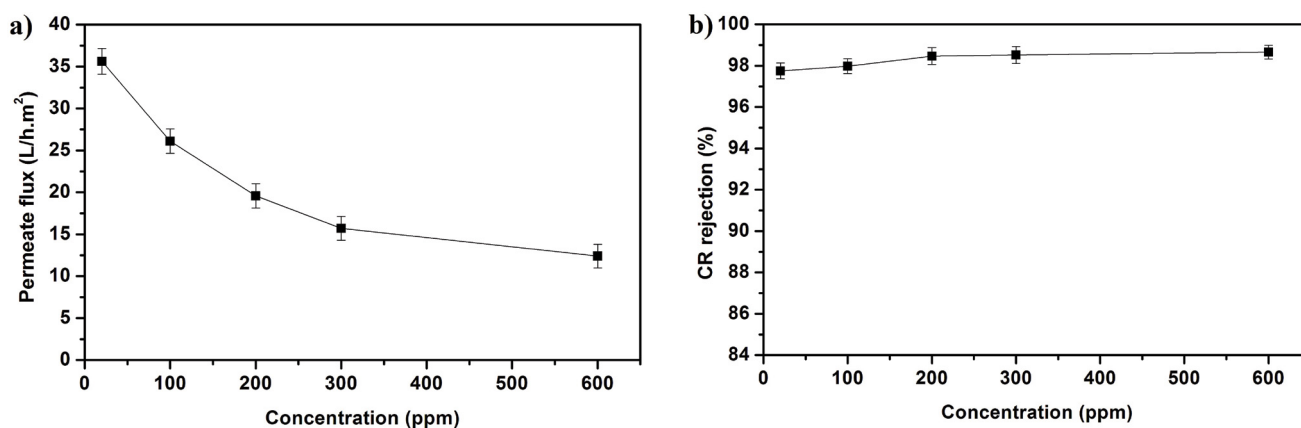


Fig. 8. CR permeate flux (a) and rejection (b) as a function of feed concentration at  $\Delta P = 3$  bar and  $\text{pH} = 6$  for 2 h of filtration.

performance towards dye filtration. In order to identify the optimum pH value, the UF experiments were investigated under an operating pressure of 3 bar, a fixed feed concentration of 600 ppm with a pH range of 4–10 during 2 h of filtration. Fig. 9 depicts the pH impact on permeate flux and the removal of CR dye. Fig. 9a shows the effect of feed pH on membrane permeate flux and indicates that it increases from 9.62 to 12.48 L/h m<sup>2</sup> as pH becomes more acidic. However, CR dye removal of 99.79% was achieved at pH 4 but only 86.17% at pH 10, as depicted in Fig. 9b. The low permeation flux and high retention under acidic conditions can be linked to the sulfonated acid groups of CR. Due to dye protonation, these groups are responsible for the decrease in the polarity and dye solubility leading to CR dye aggregation and precipitation, with concurrent membrane fouling [4]. Besides, under the same conditions, the CR dye rejection increases significantly owing to the phenomenon of polarization.

The PoPD-PVA/Pz-MP membrane has a positive charge below the point of zero charge at a pH of 6.72 ( $\text{pH}_{\text{pzc}}$ ) and therefore interacts with anionic dyes. The negatively charged ions of the CR dye are attracted by the membrane surface due to the electrostatic attractions. This results in the formation of a polarization layer [46]. Note that, as

both CR molecules and the surface layer of these particles are negative, the attraction between them provides repulsion. At basic conditions, the permeate flux goes up and CR rejection declines. The plausible explanation for these observations is weakened electrostatic attractions between dye molecules and the PoPD-PVA/Pz-MP membrane surface [46]. Therefore, pH of 4 was deemed to be the optimum pH for CR removal using the PoPD-PVA/Pz-MP membrane in this study.

### 3.3. Antifouling study

The antifouling performance is an essential criterion to examine the PoPD-PVA/Pz-MP membrane effectiveness. This study measured different antifouling properties (FRR, TFR, RFR and IFR) of the UF membrane. Water permeate and CR solution flux as well as the antifouling indexes of PoPD-PVA/Pz-MP membrane were investigated and are shown in Fig. 10. Fig. 10a shows that, compared to water flux (time = 1–120 min), filtration resulted in a significant decrease of flux (time = 140–240 min) and then, after cleaning, resulted in partial recovery of the flux (time = 260–360 min). This decrease is due to the polarization layer formed with blocked pores as well as the adsorption of the

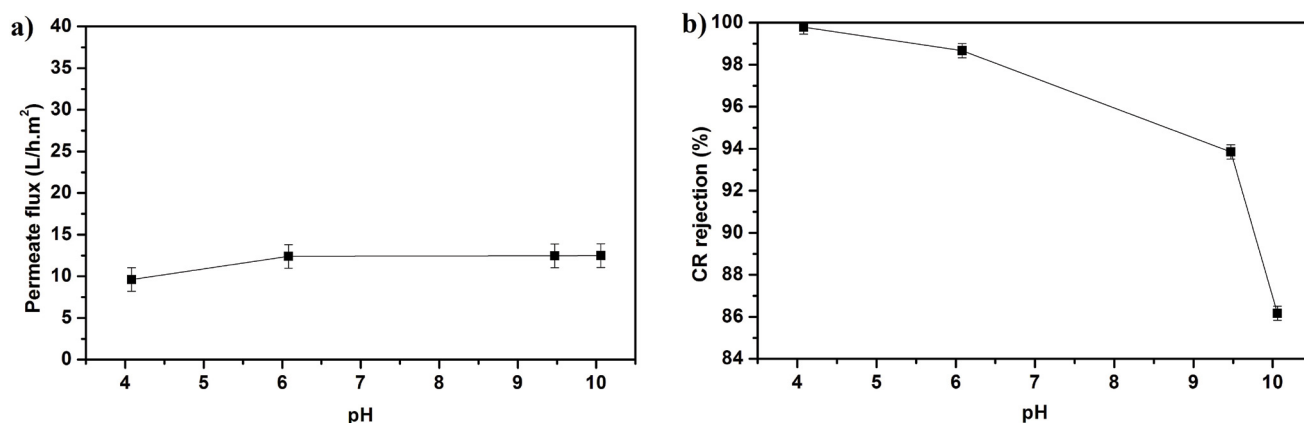


Fig. 9. CR permeate flux (a) and rejection (b) as a function of feed pH at  $\Delta P = 3$  bar and  $C = 600$  ppm for 2 h of filtration.

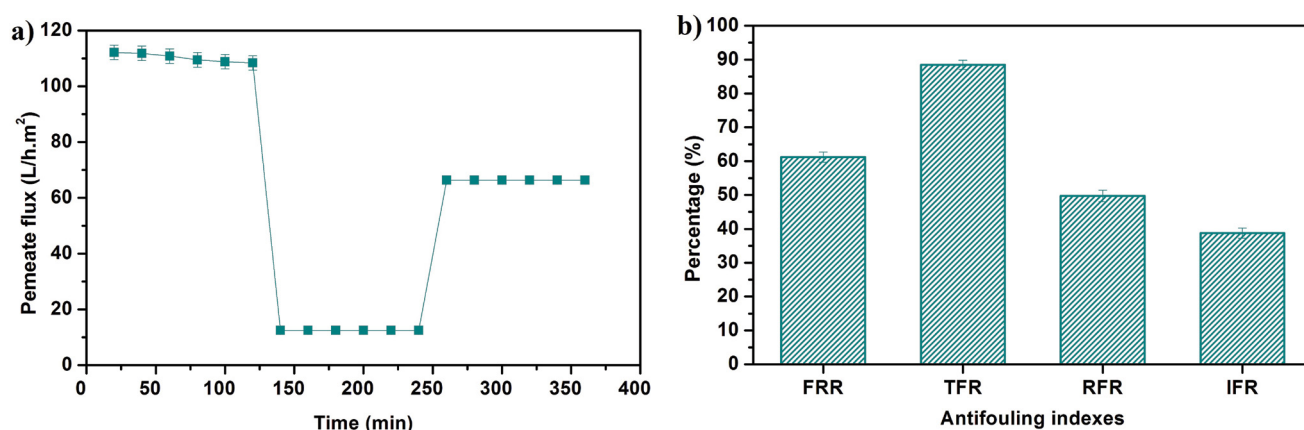


Fig. 10. (a) Permeate flux during filtration experiments and (b) antifouling parameters of PoPD-PVA/Pz-MP membrane.

CR dye on the surface of the membrane. After the physical cleaning, the permeate flux recovered significantly.

As depicted in Fig. 10b, the permeate flux of the developed membrane recovers to 61.22% (FRR = 61.22%) of the initial flux. The obtained value for TFR is 88.48%. This rate indicates that molecules in the feed accumulated and adsorbed onto the surface of the UF membrane, leading to fouling. In addition, the RFR reaches a value of 49.71%, showing that removal of the adsorbed particles from the membrane surface can be achieved by simple hydraulic washings. However, the irreversible fouling can be calculated by the IFR is about 38.77%. Recovery of this amount of flux can be achieved only by chemical cleaning since it likely involves pore blockage [53]. From these findings, the attractive antifouling parameters attest to the efficiency of the developed membrane and its potential for real-scale application.

#### 4. Conclusion

This study shows that a composite membrane was effectively prepared from PoPD and PVA on ceramic support and effectively removed CR dye from water. The polymers were coated on the Pz/MP support using the dip-coating technique. FTIR confirmed the formation of PoPD and the

co-deposited membrane selective layer (PoPD/PVA). SEM images showed that the morphology of the CM is uniform and does not exhibit any defects and has good adherence on the support. Furthermore, the developed membrane has an average pore size of 45 nm, water permeability of 37.28 L/h m<sup>2</sup> bar and WCA value of 50°. The optimized conditions for CR dye removal in terms of operating pressure, feed concentration and feed pH were determined. The rejection of UF membrane reached 99.79% at 600 ppm in acidic medium (pH = 4) under an operating pressure of 3 bar. Moreover, the developed UF membrane presents attractive antifouling characteristics. Finally, the obtained findings suggest that the developed UF membrane in this work might be effective to remove soluble, anionic dyes from industrial wastewater.

#### Acknowledgments

This work was supported the Moroccan institution of "Hassan II Academy of Science and Technology" ID: ELA5580689, for their financial support. Project name: "Multidisciplinary research on geomaterials and the volcanic geosites of Morocco: Need for their valorization and their utilization in the perspective of a sustainable development".

The authors would like to thank UARTS (Unité d'Appui Technique à la Recherche Scientifique) Rabat – Morocco for physicochemical analyses. JAC gratefully acknowledges the Lake Forest College sabbatical program and support from the J. William Fulbright Foreign Scholarship Board.

## References

- [1] Y.-Y. Su, X. Yan, Y. Chen, X.-J. Guo, X.-F. Chen, W.-Z. Lang, Facile fabrication of COF-LZU1/PES composite membrane via interfacial polymerization on microfiltration substrate for dye/salt separation, *J. Membr. Sci.*, 618 (2021) 118706, doi: 10.1016/j.memsci.2020.118706.
- [2] H. Isawi, Evaluating the performance of different nano-enhanced ultrafiltration membranes for the removal of organic pollutants from wastewater, *J. Water Process Eng.*, 31 (2019) 100833, doi: 10.1016/j.jwpe.2019.100833
- [3] Y. Zhang, W. Yu, R. Li, Y. Xu, L. Shen, H. Lin, B.-Q. Liao, G. Wu, Novel conductive membranes breaking through the selectivity-permeability trade-off for Congo red removal, *Sep. Purif. Technol.*, 211 (2019) 368–376.
- [4] C. Yang, W. Xu, Y. Nan, Y. Wang, Y. Hu, C. Gao, X. Chen, Fabrication and characterization of a high performance polyimide ultrafiltration membrane for dye removal, *J. Colloid Interface Sci.*, 562 (2020) 589–597.
- [5] V. Sri Devi, B. Sudhakar, K. Prasad, P. Jeremiah Sunadh, M. Krishna, Adsorption of Congo red from aqueous solution onto *Antigonon leptopus* leaf powder: equilibrium and kinetic modeling, *Mater. Today Proc.*, 26 (2020) 3197–3206.
- [6] P. Debnath, N.K. Mondal, Effective removal of Congo red dye from aqueous solution using biosynthesized zinc oxide nanoparticles, *Environ. Nanotechnol. Monit. Manage.*, 14 (2020) 100320, doi: 10.1016/j.enmm.2020.100320.
- [7] B. Shi, G. Li, D. Wang, C. Feng, H. Tang, Removal of direct dyes by coagulation: the performance of preformed polymeric aluminum species, *J. Hazard. Mater.*, 143 (2007) 567–574.
- [8] E. Guibal, J. Roussy, Coagulation and flocculation of dye-containing solutions using a biopolymer (Chitosan), *React. Funct. Polym.*, 67 (2007) 33–42.
- [9] M.J. Iqbal, M.N. Ashiq, Adsorption of dyes from aqueous solutions on activated charcoal, *J. Hazard. Mater.*, 139 (2007) 57–66.
- [10] A. Balcha, O.P. Yadav, T. Dey, Photocatalytic degradation of methylene blue dye by zinc oxide nanoparticles obtained from precipitation and sol-gel methods, *Environ. Sci. Pollut. Res.*, 23 (2016) 25485–25493.
- [11] P.K. Malik, S.K. Saha, Oxidation of direct dyes with hydrogen peroxide using ferrous ion as catalyst, *Sep. Purif. Technol.*, 31 (2003) 241–250.
- [12] K. Xiao, J. Sun, Y. Mo, Z. Fang, P. Liang, X. Huang, J. Ma, B. Ma, Effect of membrane pore morphology on microfiltration organic fouling: PTFE/PVDF blend membranes compared with PVDF membranes, *Desalination*, 343 (2014) 217–225.
- [13] Y. Orooji, F. Liang, A. Razmjou, S. Li, M.R. Mofid, Q. Liu, K. Guan, Z. Liu, W. Jin, Excellent biofouling alleviation of thermoexfoliated vermiculite blended poly(ether sulfone) ultrafiltration membrane, *ACS Appl. Mater. Interfaces*, 9 (2017) 30024–30034.
- [14] N. Nikooe, E. Saljoughi, Preparation and characterization of novel PVDF nanofiltration membranes with hydrophilic property for filtration of dye aqueous solution, *Appl. Surf. Sci.*, 413 (2017) 41–49.
- [15] S. Chatterjee, N. Guha, S. Krishnan, A.K. Singh, P. Mathur, D.K. Rai, Selective and recyclable Congo red dye adsorption by spherical Fe<sub>3</sub>O<sub>4</sub> nanoparticles functionalized with 1,2,4,5-benzenetetracarboxylic acid, *Sci. Rep.*, 10 (2020) 111, doi: 10.1038/s41598-019-57017-2.
- [16] U. Sathya, M. Nithya, Keerthi, Fabrication and characterisation of fine-tuned polyetherimide (PEI)/WO<sub>3</sub> composite ultrafiltration membranes for antifouling studies, *Chem. Phys. Lett.*, 744 (2020) 137201, doi: 10.1016/j.cplett.2020.137201.
- [17] Z. Chu, K. Chen, C. Xiao, H. Ling, Z. Hu, Performance improvement of polyethersulfone ultrafiltration membrane containing variform inorganic nano-additives, *Polymer*, 188 (2020) 122160, doi: 10.1016/j.polymer.2020.122160.
- [18] M. Jiang, K. Ye, J. Lin, X. Zhang, W. Ye, S. Zhao, B. Van der Bruggen, Effective dye purification using tight ceramic ultrafiltration membrane, *J. Membr. Sci.*, 566 (2018) 151–160.
- [19] Y. Kang, S. Jiao, Y. Zhao, B. Wang, Z. Zhang, W. Yin, Y. Tan, G. Pang, High-flux and high rejection TiO<sub>2</sub> nanofibers ultrafiltration membrane with porous titanium as supporter, *Sep. Purif. Technol.*, 248 (2020) 117000, doi: 10.1016/j.seppur.2020.117000.
- [20] D.Y. Koseoglu-Imer, B.K. Mutlu, M. Altinbas, I. Koyuncu, The production of polysulfone (PS) membrane with silver nanoparticles (AgNP): physical properties, filtration performances, and biofouling resistances of membranes, *J. Membr. Sci.*, 428 (2013) 620–628.
- [21] T. Mohammadi, E. Saljoughi, Effect of production conditions on morphology and permeability of asymmetric cellulose acetate membranes, *Desalination*, 243 (2009) 1–7, doi: 10.1016/j.desal.2008.04.010.
- [22] P. Daraei, N. Ghaemi, H. Sadeghi Ghari, An ultra-antifouling polyethersulfone membrane embedded with cellulose nanocrystals for improved dye and salt removal from water, *Cellulose*, 24 (2017) 915–929.
- [23] W. Li, Z. Yang, Q. Meng, C. Shen, G. Zhang, Thermally stable and solvent resistant self-crosslinked TiO<sub>2</sub>/PAN hybrid hollow fiber membrane fabricated by mutual supporting method, *J. Membr. Sci.*, 467 (2014) 253–261.
- [24] Y. Hu, M. Yue, F. Yuan, L. Yang, C. Chen, D. Sun, Bio-inspired fabrication of highly permeable and anti-fouling ultrafiltration membranes based on bacterial cellulose for efficient removal of soluble dyes and insoluble oils, *J. Membr. Sci.*, 621 (2021) 118982, doi: 10.1016/j.memsci.2020.118982.
- [25] X. Huang, C. Tian, H. Qin, W. Guo, P. Gao, H. Xiao, Preparation and characterization of Al<sup>3+</sup>-doped TiO<sub>2</sub> tight ultrafiltration membrane for efficient dye removal, *Ceram. Int.*, 46 (2020) 4679–4689.
- [26] R. Ahmad, J. Guo, J. Kim, Structural characteristics of hazardous organic dyes and relationship between membrane fouling and organic removal efficiency in fluidized ceramic membrane reactor, *J. Cleaner Prod.*, 232 (2019) 608–616.
- [27] S. Saja, A. Bouazizi, B. Achiou, H. Ouaddari, A. Karim, M. Ouammou, A. Aaddane, J. Bennazha, S. Alami Younssi, Fabrication of low-cost ceramic ultrafiltration membrane made from bentonite clay and its application for soluble dyes removal, *J. Eur. Ceram. Soc.*, 40 (2020) 2453–2462.
- [28] D. Beqqour, B. Achiou, A. Bouazizi, H. Ouaddari, H. Elomari, M. Ouammou, J. Bennazha, S. Alami Younssi, Enhancement of microfiltration performances of pozzolan membrane by incorporation of micronized phosphate and its application for industrial wastewater treatment, *J. Environ. Chem. Eng.*, 7 (2019) 102981, doi: 10.1016/j.jece.2019.102981.
- [29] A. Bouazizi, M. Breida, A. Karim, B. Achiou, M. Ouammou, J.I. Calvo, A. Aaddane, K. Khiat, S.A. Younssi, Development of a new TiO<sub>2</sub> ultrafiltration membrane on flat ceramic support made from natural bentonite and micronized phosphate and applied for dye removal, *Ceram. Int.*, 43 (2017) 1479–1487.
- [30] J. Stejskal, Polymers of phenylenediamines, *Prog. Polym. Sci.*, 41 (2015) 1–31.
- [31] J. Han, J. Dai, R. Guo, Highly efficient adsorbents of poly(o-phenylenediamine) solid and hollow sub-microspheres towards lead ions: a comparative study, *J. Colloid Interface Sci.*, 356 (2011) 749–756.
- [32] X.-G. Li, X.-L. Ma, J. Sun, M.-R. Huang, Powerful reactive sorption of silver(I) and mercury(II) onto poly(o-phenylenediamine) microparticles, *Langmuir*, 25 (2009) 1675–1684.
- [33] Z. Wang, F. Liao, Synthesis of poly(ortho-phenylenediamine) fluffy microspheres and application for the removal of Cr(VI), *J. Nanomater.*, 2012 (2012) 1–7.
- [34] S. Sakarkar, S. Muthukumar, V. Jegatheesan, Evaluation of polyvinyl alcohol (PVA) loading in the PVA/titanium dioxide (TiO<sub>2</sub>) thin film coating on polyvinylidene fluoride (PVDF)

- membrane for the removal of textile dyes, *Chemosphere*, 257 (2020) 127144, doi: 10.1016/j.chemosphere.2020.127144.
- [35] D. Beqqour, W. Taanaoui, M. Ouammou, S. Alami Younssi, J. Bennazha, J.A. Cody, M. El Rhazi, Removal of Congo red dye by ultrafiltration composite membrane of PpPD/PVA on flat pozzolan/micronized phosphate ceramic support, *Desal. Water Treat.*, 240 (2021) 165–176.
- [36] D. Beqqour, G. Derouich, W. Taanaoui, A. Essate, M. Ouammou, S. Alami Younssi, J. Bennazha, J.A. Cody, M. El Rhazi, Development of composite ultrafiltration membrane made of PmPD/PVA layer deposited on ceramic pozzolan/micronized phosphate support and its application for Congo red dye removal, *Desal. Water Treat.*, 240 (2021) 152–164.
- [37] A.M. Isloor, M.C. Nayak, Inamuddin, B. Prabhu, N. Ismail, A.F. Ismail, A.M. Asiri, Novel polyphenylsulfone (PPSU)/nano tin oxide (SnO<sub>2</sub>) mixed matrix ultrafiltration hollow fiber membranes: fabrication, characterization and toxic dyes removal from aqueous solutions, *React. Funct. Polym.*, 139 (2019) 170–180.
- [38] N. Fayoud, S. Tahiri, S. Alami Younssi, A. Albizane, D. Gallart-Mateu, M.L. Cervera, M. de la Guardia, Kinetic, isotherm and thermodynamic studies of the adsorption of methylene blue dye onto agro-based cellulosic materials, *Desal. Water Treat.*, 57 (2016) 16611–16625.
- [39] A. Kharazmi, N. Faraji, R. Mat Hussin, E. Saion, W.M.M. Yunus, K. Behzad, Structural, optical, opto-thermal and thermal properties of ZnS–PVA nanofluids synthesized through a radiolytic approach, *Beilstein J. Nanotechnol.*, 6 (2015) 529–536.
- [40] N.V. Bhat, M.M. Nate, M.B. Kurup, V.A. Bambole, S. Sabharwal, Effect of  $\gamma$ -radiation on the structure and morphology of polyvinyl alcohol films, *Nucl. Instrum. Methods Phys. Res., Sect. B*, 237 (2005) 585–592.
- [41] Y. Chen, S. Xu, S. Han, S. Chu, L. Yang, C. Jiang, Reusable and removable PmPD/PVA membrane for effective Cr(VI) adsorption and reduction, *New J. Chem.*, 43 (2019) 5039–5046.
- [42] T. Li, C. Yuan, Y. Zhao, Q. Chen, M. Wei, Y. Wang, Facile synthesis and characterization of poly(o-phenylenediamine) submicrospheres doped with glycine, *J. Macromol. Sci. Part A*, 50 (2013) 330–333.
- [43] X. Lu, H. Mao, D. Chao, X. Zhao, W. Zhang, Y. Wei, Preparation and characterization of poly(o-phenylenediamine) microrods using ferric chloride as an oxidant, *Mater. Lett.*, 61 (2007) 1400–1403.
- [44] Q. Hao, B. Sun, X. Yang, L. Lu, X. Wang, Synthesis and characterization of poly(o-phenylenediamine) hollow multi-angular microrods by interfacial method, *Mater. Lett.*, 63 (2009) 334–336.
- [45] T. Siva, K. Kamaraj, V. Karpakam, S. Sathiyarayanan, Soft template synthesis of poly(o-phenylenediamine) nanotubes and its application in self healing coatings, *Prog. Org. Coat.*, 76 (2013) 581–588.
- [46] G. Derouich, S. Alami Younssi, J. Bennazha, J.A. Cody, M. Ouammou, M. El Rhazi, Development of low-cost polypyrrole/sintered pozzolan ultrafiltration membrane and its highly efficient performance for Congo red dye removal, *J. Environ. Chem. Eng.*, 8 (2020) 103809, doi: 10.1016/j.jece.2020.103809.
- [47] F.J. Benitez, J.L. Acero, F.J. Real, C. Garcia, Removal of phenylurea herbicides in ultrapure water by ultrafiltration and nanofiltration processes, *Water Res.*, 43 (2009) 267–276.
- [48] H. Elomari, B. Achiou, D. Beqqour, K. Khaless, R. Beniazza, M. Ouammou, A. Aaddane, S. Alami Younssi, R. Benhida, Preparation and characterization of low-cost zirconia/clay membrane for removal of acid orange 74 dye, *Mater. Today Proc.*, (2021), doi: 10.1016/j.matpr.2021.03.674 (in Press).
- [49] R.V. Kumar, A.K. Ghoshal, G. Pugazhenti, Fabrication of zirconia composite membrane by in-situ hydrothermal technique and its application in separation of methyl orange, *Ecotoxicol. Environ. Saf.*, 121 (2015) 73–79.
- [50] S.M.K. Sadr, D.P. Saroj, Chapter 14 – Membrane Technologies for Municipal Wastewater Treatment, A. Basile, A. Cassano, N.K. Rastogi, Eds., *Advances in Membrane Technologies for Water Treatment: Materials, Processes and Applications*, Woodhead Publishing Series in Energy, Elsevier, 2015, pp. 443–463.
- [51] J. Lin, W. Ye, M.-C. Baltaru, Y.P. Tang, N.J. Bernstein, P. Gao, S. Balta, M. Vlad, A. Volodin, A. Sotto, P. Luis, A.L. Zydney, B. Van der Bruggen, Tight ultrafiltration membranes for enhanced separation of dyes and Na<sub>2</sub>SO<sub>4</sub> during textile wastewater treatment, *J. Membr. Sci.*, 514 (2016) 217–228.
- [52] K. Hamada, H. Nonogaki, Y. Fukushima, B. Munkhbat, M. Mitsuishi, Effects of hydrating water molecules on the aggregation behavior of azo dyes in aqueous solutions, *Dyes Pigm.*, 16 (1991) 111–118.
- [53] C. Lavanya, K. Soontarapa, M.S. Jyothi, R. Geetha Balakrishna, Environmental friendly and cost effective caramel for Congo red removal, high flux, and fouling resistance of polysulfone membranes, *Sep. Purif. Technol.*, 211 (2019) 348–358.